Chemical Engineering Journal 147 (2009) 71–78

Contents lists available at ScienceDirect

Chemical Engineering Journal

journal homepage: www.elsevier.com/locate/cej

Synthesis of iron oxide nanorods and nanocubes in an imidazolium ionic liquid

Yong Wang, Hong Yang*

Department of Chemical Engineering, University of Rochester, Gavett Hall 206, Rochester, NY 14627, USA

ARTICLE INFO

Keywords:
Nanorod
Nanocube
Ionic liquid
Imidazolium
[BMIM][Tf_2N]
Iron oxide
Iron carbonyl

ABSTRACT

This paper reports the synthesis of iron oxide nanostructures with well-defined shapes, including rod, cube, and sphere, in 1-butyl-3-methylimidazolium bis(triflylmethyl-sulfonyl) imide ([BMIM][Tf_2N]) ionic liquid (IL). Surfactants including oleic acid and oleylamine, which are commonly used as surface capping agents for size and shape control in molecular solvents, can be employed for making morphologically well-defined nanostructures in this IL. Iron pentacarbonyl thermally decomposes at elevated temperatures in [BMIM][Tf_2N] ionic liquid and subsequently form nanoparticles. Nanorods, nanocubes, and spherical particles were synthesized depending mainly on the reaction temperatures and surfactants. X-ray diffraction and transmission electron microscopy data indicated these nanostructures were largely cubic iron oxide, maghemite. Our results show that imidazolium-based ionic liquids can be used as solvent for achieving very high level control over the size and shape of nanostructures. The approach developed in this work can potentially be used as a viable method for making various other uniform nanostructures in ionic liquids.

1. Introduction

This paper presents the synthesis of cubic and rod-shaped nanostructures of iron oxide in 1-butyl-3-methylimidazolium bis(triflylmethyl-sulfonyl) imide ([BMIM][Tf_2N]) ionic liquid (IL). Oleic acid and oleyamine, which are commonly used capping agents for the shape control of nanomaterials made in molecular solvents, are found to be very effective in making nanorods and nanocubes of iron oxide from iron pentacarbonyl precursor in this IL.

The application of ionic liquid as solvent for making nanoparticles has attracted a lot of attentions in the past several years [1–5]. In comparison to molecular solvents, ionic liquids can have quite different solvation properties in that they can have extended hydrogen bonds and large ionic strength [6–8]. Such property suggests that cage-like nanostructures are possible for ionic liquids and used as confined reaction environments in the synthesis [3,9,10]. There are two major approaches for making nanostructured materials in ionic liquids depending on the use of capping agents. Most of research work in this area has been focused on the direct application of ionic liquid without addition of capping agents [3,4,11–16], although such reagents are commonly used for making nanomaterials in molecular solvents [2,17–25]. Recently reported nanomaterials made in IL media have expanded rapidly from noble metals to oxides, fluorides and other more complex compositions [1,4,13,26–29], and some levels of shape control have also been achieved [1,4,5,16,30–32]. Among the various ILs, imidazolium-based compounds are the most commonly used solvents [4,5,12,13,33–37]. While the formation mechanism of nanoparticles is largely unclear and required further study, a few latest reports suggest that the cage-like assemblies of ionic liquid components, which are hydrogen-bonded and analogous to the micellular structures in conventional solvent systems [9,10,38]. This ordered structure might also relate to the observation that nanoparticles generated directly in ionic liquids are typically quite small and below 5 nm in diameter. So far, however, the size and shape of nanostructures cannot be readily controlled well in such reaction systems except spherical particles. It would greatly increase the impact of ionic liquids as solvents in processing nanomaterials if those strategies used for controlling monodispersity and morphology in molecular solvents can be developed for ionic liquid systems.

In this work, we present the use of surface capping agents in controlling the morphology of nanoparticles, as these chemicals play essential roles in making nanostructures of various shapes in different molecular solvents [17–20]. Among the large pool of candidates for capping agents, oleic acid and oleylamine have been selected, because they both are widely used in making nanowires and several other shapes [2,39,40]. Furthermore, our previous studies show that these surfactants can be good capping agents for the synthesis of monodispersed nanoparticles of silver, platinum and iron oxides in the [BMIM][Tf_2N] ionic liquid [5,33,34]. Finally, iron oxides have been chosen as our targeted materials, because they have been widely used in biological applications as magnetic contrast agents [2] and a commonly used precursor, iron pentacarbonyl, can dissolve very well in [BMIM][Tf_2N] IL [33].

* Corresponding author. Tel.: +1 585 275 2110; fax: +1 585 473 1348.
E-mail address: hongyang@che.rochester.edu (H. Yang).

1385-8947/$ – see front matter © 2008 Elsevier B.V. All rights reserved.
doi:10.1016/j.cej.2008.11.043

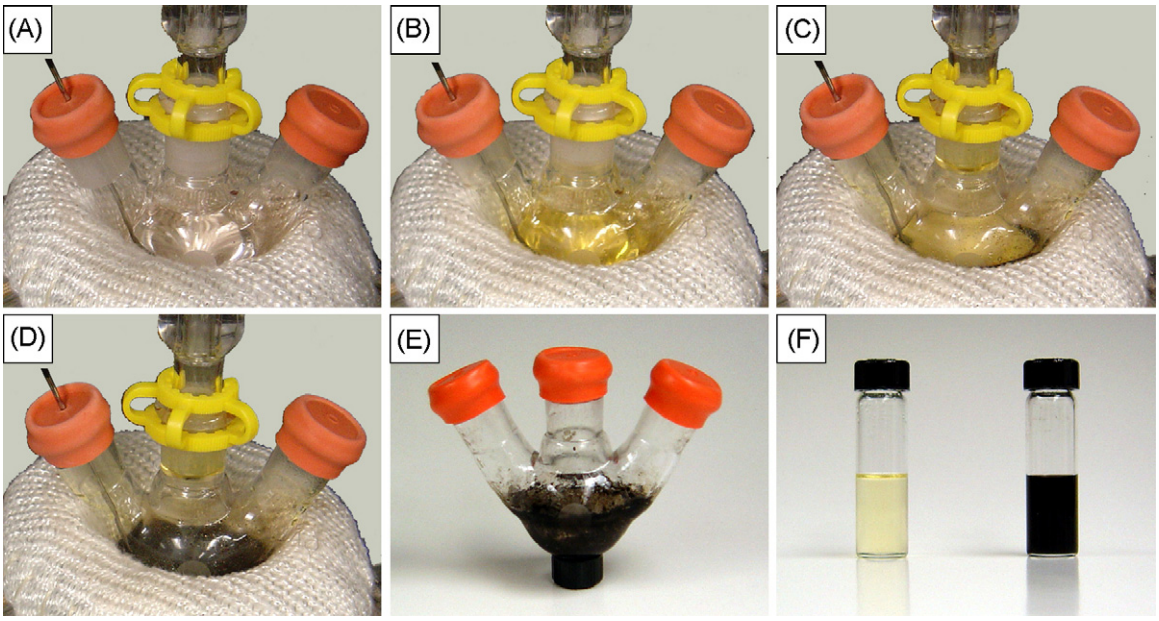

Fig. 1. Photographs of reaction process in [BMIM][Tf_2N] IL: (A) IL containing oleic acid at 110 °C, the reaction mixture (B) at 110 °C after the injection of $Fe(CO)_5$, at (C) 200 °C and (D) ~204 °C showing the color change, (E) the nanomaterials deposited on the wall of flask after the reaction and removal of IL, and (F) the IL after reaction (the vial on the left) and the final product dispersed in hexane (the vial on the right).

2. Experimental

2.1. Materials

Iron pentacarbonyl (99.999%), oleic acid (99.99%), oleylamine (70%, tech. grade), 1,2-hexadecanediol (90%, tech. grade), hexane (anhydrous, 95+%), and lithium bistrifluoromethanesulfonimidate (≥99.95%) were provided by Aldrich. Acetone (HPLC grade), chlorobutane (99.5+%), and 1-methylimidazole (99%) were purchased from VWR. All reagents and chemicals were used as received without further purifications. [BMIM][Tf_2N] ionic liquid was made in-house following a procedure reported elsewhere [5,6]. Its structure was confirmed by nuclear magnetic resonance (NMR). The water content in [BMIM][Tf_2N] was about 0.03%, as determined by Karl Fisher coulommetry. The chlorine contents were not detectable (<0.3 wt%) using potentiometric titration with silver nitrate.

2.2. General synthesis and separation procedures

In a typical synthesis of iron oxide nanoparticles, freshly dried [BMIM][Tf_2N] was mixed with predetermined amount of oleic acid, oleylamine and 1,2-hexandecandiol in a 15-mL three-neck flask. This mixture was heated with a heating mantle under argon and stirred vigorously by a magnetic stirrer. The mixture turned into a colorless transparent solution at 75 °C after 1,2-hexandecandiol was dissolved. Iron pentacarbonyl was then added into the flask at 110 °C using a micro-syringe (*Caution*: iron pentacarbonyl is flammable and toxic. It should be handled with care in a fume hood or glove box). This reaction mixture was heated to and kept at a predetermined temperature for a given period of time before the reaction was terminated by removing the heating source. After the mixture cooled down, the ionic liquid in the reaction vessel was then collected using a pipette. The product, a black solid, was extracted by washing with hexane which contained small amount of oleic acid and oleylamine. The nanorods were collected by centrifugation. The suspension of such nanomaterials in hexane was diluted with additional hexane and then centrifuged for 10 min. The black precipitation was discarded and the supernatant was centrifugated again. The resultant black precipitate was collected as the final product.

2.3. Synthesis of nanorods

The mixture for the synthesis of iron oxide nanorods contained 5 mL of freshly dried [BMIM][Tf_2N], 40 μL (0.13 mmol) of oleic acid, 43 μL (0.09 mmol) of oleylamine and 98 mg of 1,2-hexandecandiol (or 0.34 mmol). The amount of iron pentacarbonyl used was 100 μL (0.75 mmol). The reaction mixture turned into dark red rapidly and became dark black when temperature reached 140 °C. This reaction mixture was heated to ~310 °C in 2 h after injection of $Fe(CO)_5$, and kept at this temperature for another 1 h before the reaction was terminated. The product was extracted by washing with 6 mL of hexane which contained 40 μL of oleic acid and 40 μL of oleylamine. After centrifugation, the suspension of such nanomaterials in hexane (0.5 mL) was diluted with additional 20 mL of hexane and then centrifuged at 1000 rpm for 10 min. The black precipitation was discarded and the supernatant was centrifugated again at 6000 rpm for 30 min.

2.4. Synthesis of 9 nm nanocubes

The typical synthetic mixture contained 5 mL of [BMIM][Tf_2N] and 80 μL of oleic acid (~0.25 mmol). The amount of iron pentacarbonyl used was 33 μL (0.25 mmol). The reaction mixture turned to light yellow after the injection. The color of the reaction mixture became completely black at ~230 °C. This reaction mixture was heated to 280 °C in 2 h from the time of adding $Fe(CO)_5$, and kept at this temperature for another 1 h before the reaction was terminated. The resulting materials deposited on the wall of the flask, and a transparent ionic liquid could be readily separated out by decantation. The solid products were easily collected by washing with 6 mL of hexane. A suspension of such nanomaterials in hexane (0.1 mL) was further diluted with 2 mL of hexane and then centrifuged at 8000 rpm for 10 min.

2.5. Synthesis of 13 nm nanocubes

The typical synthetic mixture contained 3 mL of [BMIM][Tf_2N] and 48 μL (0.15 mmol) of oleic acid. The amount of iron pentacarbonyl used was 60 μL (0.45 mmol). The reaction mixture turned

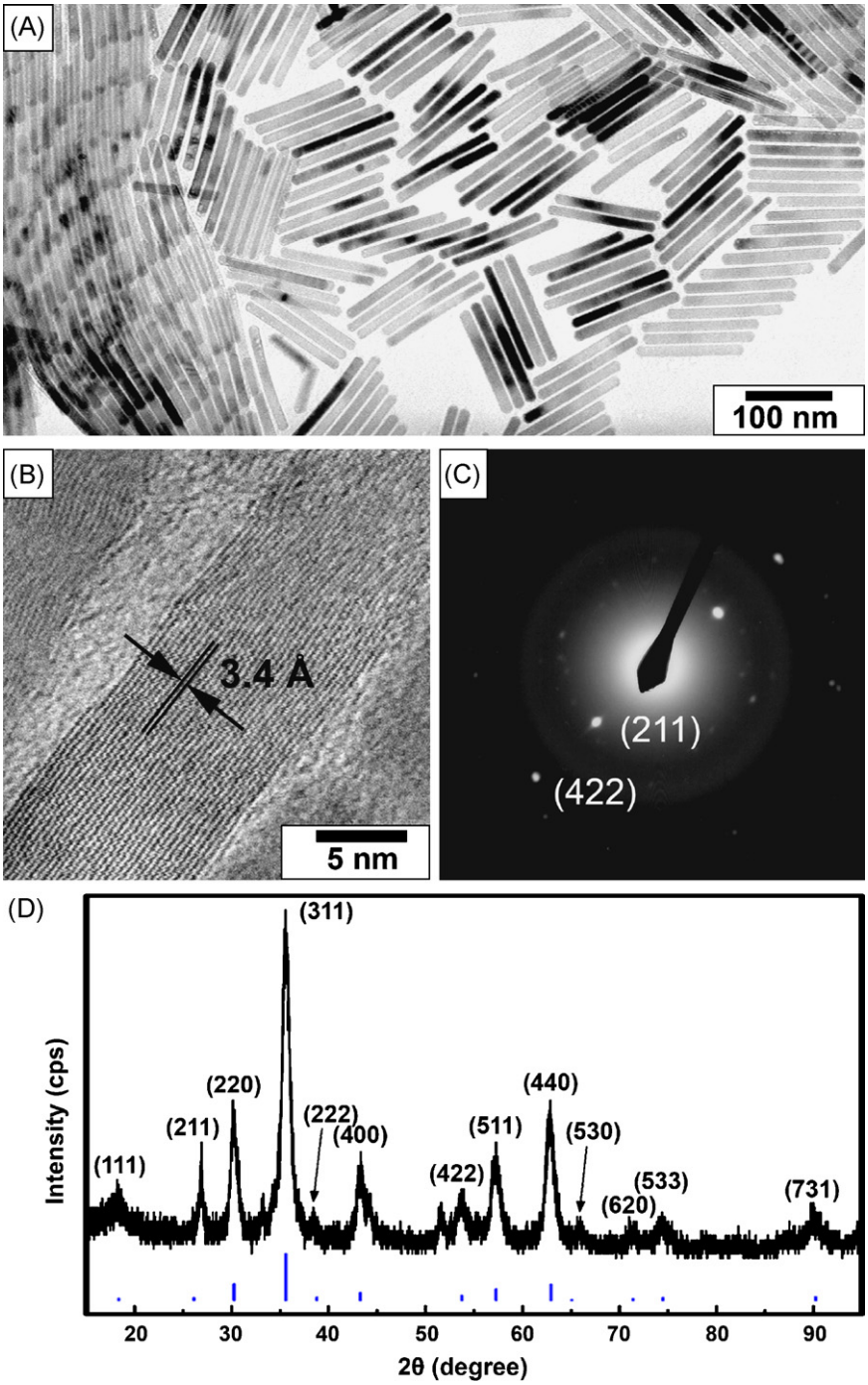

Fig. 2. (A and B) TEM images, (C) SAED, and (D) PXRD patterns of iron oxide nanorods made at $Fe(CO)_5$ concentration of 0.15 M and $Fe(CO)_5$:1,2-hexadecanediol:oleic acid:oleylamine molar ratio of 6:2.7:1:0.7. The reaction temperature was 310 °C. The SAED pattern was mostly from a single nanorod. The lines in Panel D indicate the position and relative intensity of the peaks for γ-Fe_2O_3 (ICDD PDF database).

to light yellow after the injection and became completely black at ~210 °C. The rest of synthesis and reaction steps were similar to those for making 9 nm nanocubes.

2.6. Characterizations

Transmission electron microscopy (TEM) images and electron diffraction (ED) patterns were recorded on a JEOL JEM 2000EX microscope at an accelerating voltage of 200 kV. High resolution TEM (HR-TEM) images were recorded on a Hitachi HD-2000 scanning transmission electron microscope (STEM) operating in ultra-high resolution mode at an accelerating voltage of 200 kV and an imaging current of 30 mA. Power X-ray diffraction (PXRD) spectra were record on a Philips MPD diffractometer with a Cu Kα X-ray source (λ = 1.54056 Å). The Fourier transform infrared (FT-IR) spectra were collected on a Nicolet 20 SXC spectrometer. The specimen was made by dropping the appropriate samples between two pieces of KBr crystals to form a thin film. The proton NMR spectra were recorded on an Avance-400 spectrometer (400 MHz). The NMR specimens were made by mixing 1.5 mg of samples with 2 mL of *d*-chloroform.

3. Results and discussion

The synthesis of iron oxide nanostructures was conducted in [BMIM][Tf_2N] ionic liquids using $Fe(CO)_5$ as precursor. Previously we showed that spherical iron oxide nanoparticles can be made in this IL and settled out when oleic acid was used as capping agent [33]. The ILs could be recovered subsequently and reused again, while the nanomaterials made were readily collected using conventional organic solvents. There were distinct stages that could be followed through the color changes of the reaction mixtures during the formation of nanostructures, as shown in Fig. 1. Typically, upon the addition of $Fe(CO)_5$ at 110 °C, the transparent colorless IL mixtures turned into light yellowish color, Fig. 1A and B. The color of this mixture turned into brown with the increase of temperature and into black quickly in the temperature range between 200 and 230 °C, indicating the early stage decomposition of $Fe(CO)_5$, Fig. 1C and D. The accumulation of solid on the reaction flask wall could be observed when the temperature reached 220 °C. The final reaction was kept at between 280 and 310 °C for 1 h depending on the final shapes. After the reaction was complete, the IL phase was almost colorless or light yellowish depending on the precursor amount and surfactants used. This IL phase could be collected by simple decantation. The used ionic liquid shown in Fig. 1F has been passed through a PTFE filter (average pore diameter: 0.2 μm). The nanomaterials deposited on the flask walls, could be readily washed out and dispersed in hexane or some other organic solvents, such as toluene and chloroform, Fig. 1F.

Nanorods were made at $Fe(CO)_5$ concentration of 0.15 M and $Fe(CO)_5$:1,2-hexadecanediol:oleic acid:oleylamine molar ratio of 6:2.7:1:0.7. The final reaction temperature was kept at 310 °C. These nanorods had an average diameter of 12 ± 2 nm and an aspect ratio of about 10 ± 1, Fig. 2A. The uniformity in both the diameter and aspect ratio could be accomplished. Some liquid crystal-like

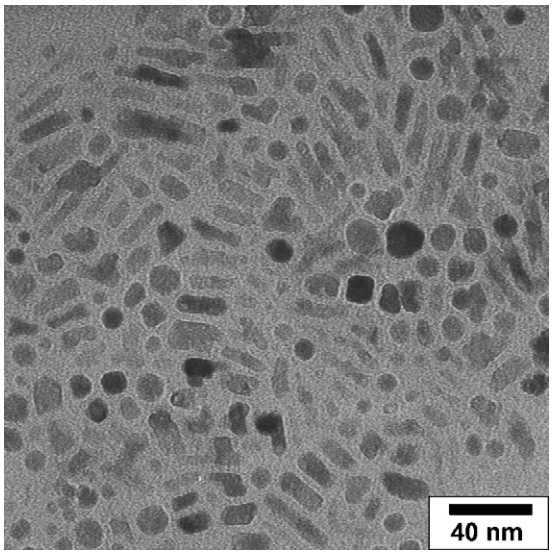

Fig. 3. Representative TEM image of nanoparticles made at $Fe(CO)_5$ concentration of 50 mM and $Fe(CO)_5$:oleic acid molar ratio of 1:1 in 5 mL of [BMIM][Tf_2N] IL. The reaction temperature was 310 °C.

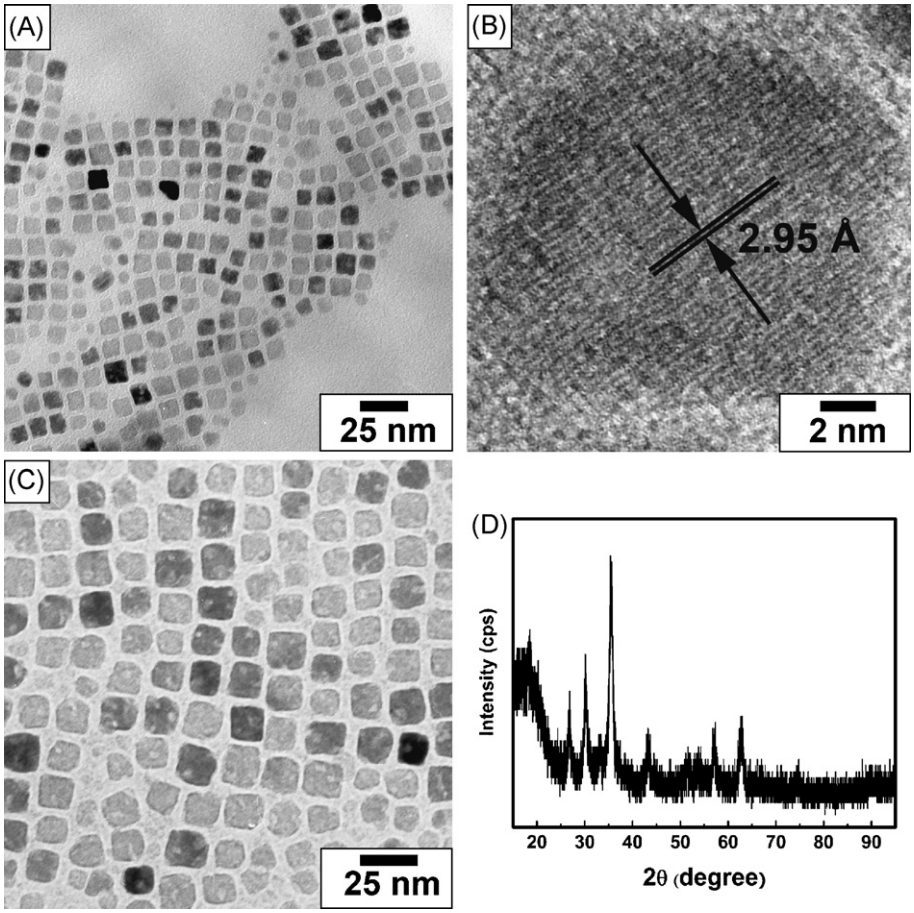

Fig. 4. (A–C) TEM images and (D) PXRD pattern of iron oxide nanocubes: (A and B) 9 nm nanocubes made from a reaction solution at $Fe(CO)_5$ concentration of 50 mM and $Fe(CO)_5$:oleic acid molar ratio of 1:1, and (C) 13 nm nanocubes from a solution at $Fe(CO)_5$ concentration of 150 mM and $Fe(CO)_5$:oleic acid molar ratio of 3:1 (C). The reaction temperature was 280 °C for both reactions.

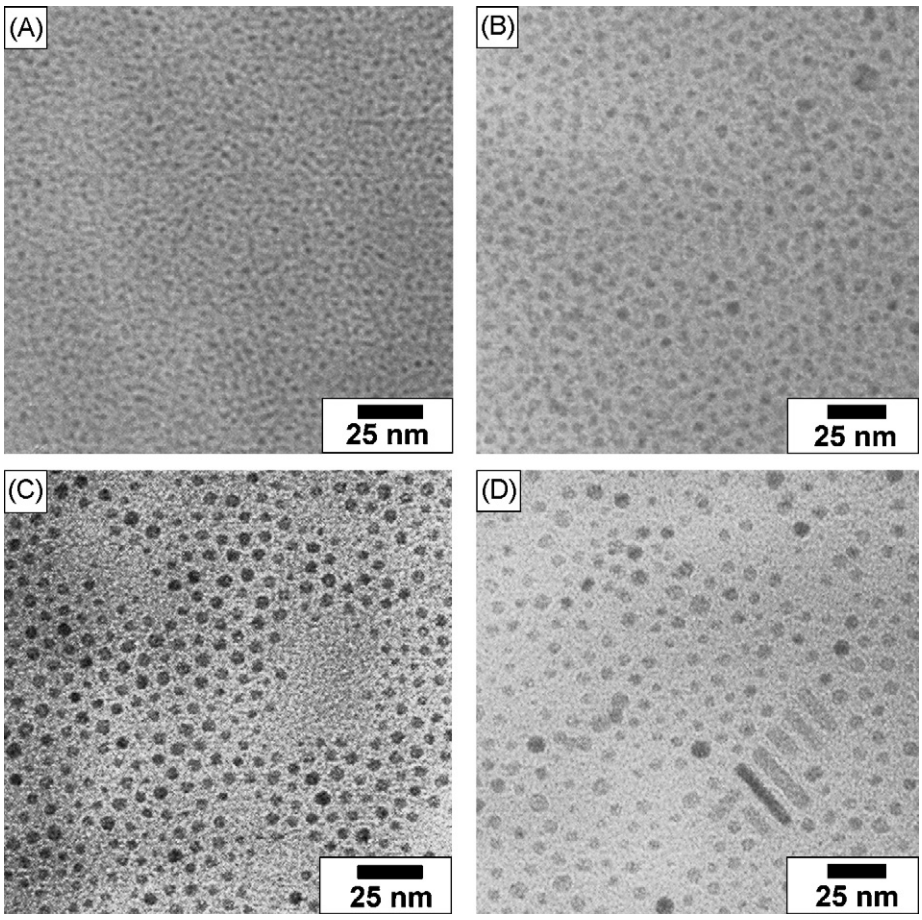

Fig. 5. TEM images showing the evolution of nanoparticles produced from a mixture of 50 mM of $Fe(CO)_5$ in 5 mL of [BMIM][Tf_2N] IL and $Fe(CO)_5$:1,2-hexadecanediol:oleic acid:oleylamine molar ratio of 2:2.7:1.6:0.3. The products were collected at (A) 270 °C after reaction for 100 min, (B) 280 °C after reaction for 110 min, (C) 288 °C after reaction for 120 min, and (D) 292 °C after reaction for 160 min.

alignment of nanorods could be observed in the self-assembled structures of nanorods in the absence of external field. HR-TEM study indicated that the nanorod was crystalline. The lattice spacing for the crystalline planes shown in Fig. 2B was 3.4 Å, which could be assigned to (2 1 1) plane of cubic γ-Fe_2O_3. This observation was supported by the observation that selected area electron diffraction (SAED) pattern on a single rod showed the diffraction from (2 1 1) planes, Fig. 2C. The PXRD data of these nanorods show that all major diffractions could be assigned to mainly γ-Fe_2O_3 (maghemite, space group: $P4_132$, ICDD PDF No. 39-1346) [41,42]. The less-oxidized form of iron oxide magnetite, which has similar XRD patterns to the cubic maghemite, could be the minor crystal phase. The formation of final maghemite could be a combination of oxidation events occurred due to the exposure of nanorods to oxygen or air. This observation on the crystalline form agreed well with other iron oxide nanoparticles previously reported [43]. The result also agreed with the reported stable phase of iron oxide in the temperature range of 200–400 °C [44]. These nanorods responded to external field in the form of suspension in hexane and could be collected using a permanent magnet with field strength of about 2 kOe. The estimated yield of nanorods was about 40% in weight based on the content of iron. The highly concentrated Fe_2O_3 nanorods with very small amount of spherical particles could be obtained through either centrifuge or magnetic separation.

Oleylamine and 1,2-hexadecanediol appeared to be important for the synthesis of Fe_2O_3 nanorods in this IL system. In the absence of oleylamine and 1,2-hexadecanediol, only low-yielded rod-like, spherical and faceted particles were obtained, Fig. 3. This observation suggests that oleic acid, while was critical in the shape control, was not enough if used alone to interact effectively with the selective low-index planes under this set of reaction condition. Previously, spherical iron oxide nanoparticles were made in the presence of oleic acid at 280 °C [33]. Addition of oleylamine to oleic acid–IL mixture could affect the size, but not shape, of the particles under similar reaction conditions. Thus, it appeared that temperature also played a critical role in controlling the kinetics of relative growth rates along different directions. The combination of changing the concentrations of capping agents and subtle variation in temperature between about 280 and 310 °C could results in the formation of iron oxide nanorods and possibly other shapes.

The observation of facets in nanoparticles suggested that preferred binding between oleic acid and selective iron oxide existed. As temperature was found to be crucial in controlling the morphology of nanocrystals, we lowered the final reaction temperature from 310 to 280 °C while maintaining all other reaction conditions and reactant ratios the same in order to increase the difference in reaction rates along various directions. Using 50 mM of $Fe(CO)_5$ in 5 mL of [BMIM][Tf_2N] IL, and $Fe(CO)_5$:oleic acid molar ratio of 1:1, we obtained nanocubes from the reactions conducted at 280 °C, Fig. 4A. The average edge length of these nanocubes was about 9 ± 1 nm. The formation of nanocubes should be due to the preferred stabilization of iron oxide {1 0 0} surfaces by oleic acid. High resolution TEM image shows the nanocubes were highly crystalline, Fig. 4B. Lattice fringe of 2.95 Å was observed along the diagonal direction of nanocubes, which could be indexed to (2 2 0) plane of γ-Fe_2O_3. These nanocubes grew in size if the $Fe(CO)_5$ oleic acid molar ratio increased from 1:1 to 3:1 while maintaining the reaction temperature at 280 °C, Fig. 4C. The PXRD pattern shows these iron oxide

nanostructures were dominated by the maghemite phase, Fig. 4D. The nanocubes made at the $Fe(CO)_5$ oleic acid molar ratio of 3:1 had an average edge length of 13 ± 2 nm, which was about 40% larger than those made with $Fe(CO)_5$ oleic acid molar ratio of 1:1. As the $Fe(CO)_5$ oleic acid ratio increased by three times, the volume change of individual nanocube grew proportionally. This observation suggested that the particle growth was mostly likely a mass transport controlled process at this condition. The estimated relative population of nanocubes was >70% in the as-made products for both cases even without the separation procedure. The other shape was found to be mostly spherical particles with diameters typically less than 4 nm.

To understand the formation of iron oxide nanostructures, we studied the reaction systems used for the synthesis of nanorods nanoparticles at early stages of the reactions. To be specific, we examined the particle formation for the mixture of $Fe(CO)_5$:1,2-hexadecanediol:oleic acid:oleylamine molar ratio of 2:2.7:1:0.7 in 5 mL of [BMIM][Tf_2N] IL and $Fe(CO)_5$ concentration of 50 mM. Similarly, black precipitation formed on the wall of reaction flask at about 220 °C. This precipitation was collected by dispersing in hexane to form a transparent brownish suspension. TEM study shows that the first set of readily observable tiny clusters formed at around 270 °C, Fig. 5A. These clusters grew in size with increase of reaction temperature and time, Fig. 5B. The well-separated nanoparticles formed when reaction temperature was about 280 °C, Fig. 5C. Nanorods began to emerge when reaction temperature was increased to above 290 °C, Fig. 5D. It seems that the nanorods formed through the growth of primary particles at the relatively low temperature. While the tiny clusters could be stable in [BMIM][Tf_2N], the large nanoparticles always settled out from the IL mixtures and grew continuously.

Fourier transform infrared and proton NMR were used to examine [BMIM][Tf_2N] and its mixtures with oleic acid and $Fe(CO)_5$. The concentrations of oleic acid and $Fe(CO)_5$ used in these tests were the same as those for the synthesis of 9 nm cubes. Fig. 6 shows the FT-IR spectra of pure [BMIM][Tf_2N], its mixture with oleic acid and $Fe(CO)_5$, and [BMIM][Tf_2N] IL recovered after the completion of reaction. Upon the addition of $Fe(CO)_5$ to [BMIM][Tf_2N] IL, the asymmetric and symmetric carbonyl stretching vibration of $Fe(CO)_5$, which were centered at 2019 and 1996 cm^{-1} in the typical hydrocarbon solvents [45], moved to 2021 and 2000 cm^{-1}, respectively. These shifts were due to the interaction between the [BMIM] cation and the carbonyl groups of $Fe(CO)_5$ [46]. The IR spectrum of the mixture after the reaction shows almost identical pattern with that of pure [BMIM][Tf_2N]. The weak and broad bands in 1780–1650 and 1540–1490 cm^{-1} could come from oleic acid residues. These IR

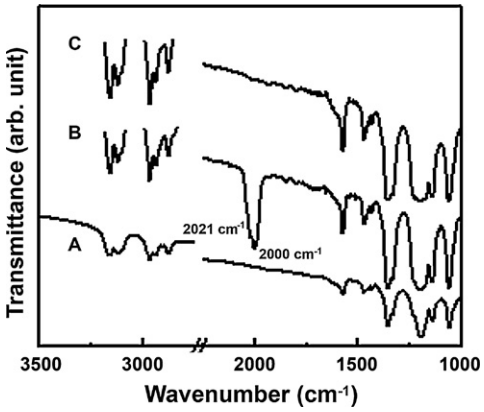

Fig. 6. FT-IR spectra of (A) pure [BMIM][Tf_2N] IL, (B) the mixture of IL and oleic acid after the addition of $Fe(CO)_5$, and (C) [BMIM][Tf_2N] IL recovered after the completion of reaction, respectively. The bands centered at 2021 and 2000 cm^{-1} were from the asymmetric and symmetric carbonyl stretching vibrations of $Fe(CO)_5$, respectively.

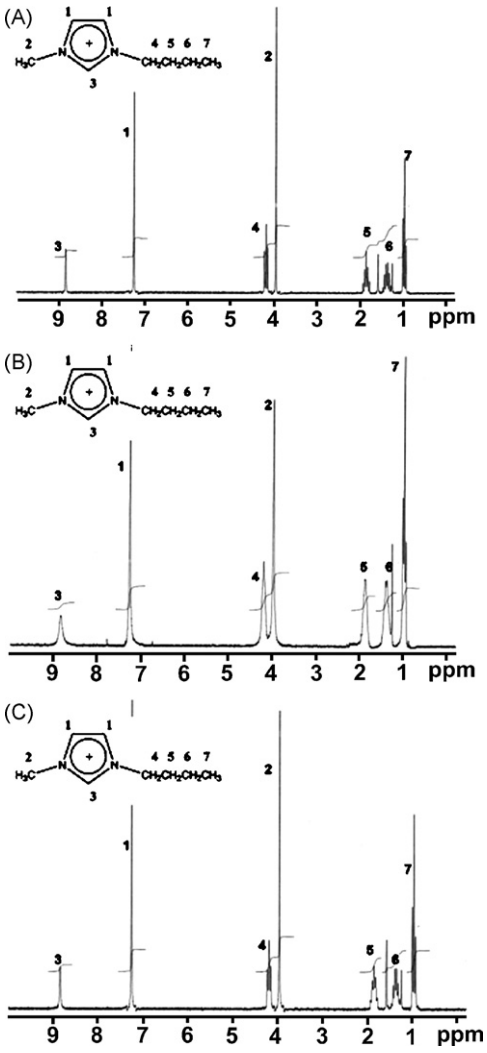

Fig. 7. Proton NMR spectra of (A) pure [BMIM][Tf_2N] IL, (B) the mixture of $Fe(CO)_5$ and oleic acid in [BMIM][Tf_2N] IL made at 110 °C, and (C) [BMIM][Tf_2N] IL after the reaction. The line-broadening and the disappearance of fine features can clearly been observed in (B).

data were in line with our NMR study. Fig. 7 shows the proton NMR spectra of the three specimens. The peaks for [BMIM][Tf_2N] became substantially broaden after the addition of $Fe(CO)_5$, Fig. 7B. A light yellowish precipitation in *d*-chloroform was observed in the NMR tube. All these observations suggested that there was a favorable interaction between [BMIM][Tf_2N] IL and $Fe(CO)_5$. The NMR spectrum of the mixture after the reaction showed an identical pattern with that of pure [BMIM][Tf_2N], Fig. 7C. The addition of oleic acid did not cause noticeable changes in either FT-IR or NMR spectra. Phase separation was also observed between [BMIM][Tf_2N] IL and oleic acid.

Based on the above observation, it appeared that the formation of nanocubes and nanorods could be related to the biphasic nature of this IL-based process and favorable solubility of $Fe(CO)_5$ in [BMIM][Tf_2N] ionic liquid [46,47]. The biphasic behavior might facilitate the separation nanoparticles formed from the IL mixtures and the delivery of reactant nutrients for growth. These nutrients could be the thermally decomposed iron-containing species from $Fe(CO)_5$ complexed with carboxylate group of oleic acid [48]. The surface capping agents did work well in this IL in helping create the large difference in reactivity among the low-index surfaces of nanocrystals and in facilitating the formation of nanocubes and nanorods. While the secondary growth of small particles in an

oriented fashion, similar to some of the rods generated through the oriented attachment [49,50], could be a possibility for the formation of nanorods, the above studies indicated that protection of (1 0 0) plane of Fe_2O_3 by oleic acid should the dominant factor in this shape-controlled reaction, particularly at reaction temperatures around 280 °C.

4. Conclusion

In conclusion, nanorods, nanocubes and nanospheres of iron oxide have been synthesized in [BMIM][Tf_2N] ionic liquid. Oleic acid plays an important role in the shape control of nanostructures. Oleylamine and 1,2-hexadecanediol are required co-surfactants in controlling the formation of nanorods of iron oxide. The different solubility of precursors, reactive intermediates and nanoparticles in ionic liquid helps to regulate the delivery of agents in different phases. This work shows that high level morphological control of nanomaterials is feasible using ionic liquids by selecting proper capping agents and reaction conditions, which is an important step forward in using ionic liquids as solvents for controlling the size and shape of nanomaterials.

Acknowledgements

This work was supported in part by the National Science Foundation (CAREER Award, DMR-0449849 and SGER Grant, CTS-041722), and the Environmental Protection Agency (R831722). The high resolution STEM was performed at the Centre for Nanostructure Imaging, University of Toronto, which is jointly funded by Canada Foundation of Innovation and Ontario Innovation Trust. We thank Dr. Marc Mamak for running the STEM.

References

[1] M. Antonietti, D.B. Kuang, B. Smarsly, Z. Yong, Ionic liquids for the convenient synthesis of functional nanoparticles and other inorganic nanostructures, Angew. Chem. Int. Ed. 43 (2004) 4988–4992.
[2] U. Jeong, X.W. Teng, Y. Wang, H. Yang, Y.N. Xia, Superparamagnetic colloids: controlled synthesis and niche applications, Adv. Mater. 19 (2007) 33–60.
[3] P. Migowski, J. Dupont, Catalytic applications of metal nanoparticles in imidazolium ionic liquids, Chem. Eur. J. 13 (2007) 32–39.
[4] A. Taubert, Z. Li, Inorganic materials from ionic liquids, Dalton Trans. (2007) 723–727.
[5] Y. Wang, H. Yang, Synthesis of CoPt nanorods in ionic liquids, J. Am. Chem. Soc. 127 (2005) 5316–5317.
[6] J.G. Huddleston, A.E. Visser, W.M. Reichert, H.D. Willauer, G.A. Broker, R.D. Rogers, Characterization and comparison of hydrophilic and hydrophobic room temperature ionic liquids incorporating the imidazolium cation, Green Chem. 3 (2001) 156–164.
[7] P. Wasserscheid, T. Welton, Ionic Liquids in Synthesis, 1st ed., Wiley–VCH, Weinheim, 2003, p. 364.
[8] G.A. Baker, S.N. Baker, S. Pandey, F.V. Bright, An analytical view of ionic liquids, Analyst 130 (2005) 800–808.
[9] T. Gutel, J. Garcia-Anton, K. Pelzer, K. Philippot, C.C. Santini, Y. Chauvin, B. Chaudret, J.M. Basset, Influence of the self-organization of ionic liquids on the size of ruthenium nanoparticles: effect of the temperature and stirring, J. Mater. Chem. 17 (2007) 3290–3292.
[10] J. Dupont, On the solid, liquid and solution structural organization of imidazolium ionic liquids, J. Braz. Chem. Soc. 15 (2004) 341–350.
[11] E. Redel, R. Thomann, C. Janiak, Use of ionic liquids (ILs) for the IL-anion size-dependent formation of Cr, Mo and W nanoparticles from metal carbonyl M(CO)(6) precursors, Chem. Commun. (2008) 1789–1791.
[12] J. Kramer, E. Redel, R. Thomann, C. Janiak, Use of ionic liquids for the synthesis of iron, ruthenium, and osmium nanoparticles from their metal carbonyl precursors, Organometallics 27 (2008) 1976–1978.
[13] G.S. Fonseca, G. Machado, S.R. Teixeira, G.H. Fecher, J. Morais, M.C.M. Alves, J. Dupont, Synthesis and characterization of catalytic iridium nanoparticles in imidazolium ionic liquids, J. Colloid Interf. Sci. 301 (2006) 193–204.
[14] H.S. Schrekker, M.A. Gelesky, M.P. Stracke, C.M.L. Schrekker, G. Machado, S.R. Teixeira, J.C. Rubim, J. Dupont, Disclosure of the imidazolium cation coordination and stabilization mode in ionic liquid stabilized gold(0) nanoparticles, J. Colloid Interf. Sci. 316 (2007) 189–195.
[15] J. Dupont, G.S. Fonseca, A.P. Umpierre, P.F.P. Fichtner, S.R. Teixeira, Transition-metal nanoparticles in imidazolium ionic liquids: recycable catalysts for biphasic hydrogenation reactions, J. Am. Chem. Soc. 124 (2002) 4228–4229.
[16] Z.G. Li, A. Friedrich, A. Taubert, Gold microcrystal synthesis via reduction of $HAuCl_4$ by cellulose in the ionic liquid 1-butyl-3-methyl imidazolium chloride, J. Mater. Chem. 18 (2008) 1008–1014.
[17] Y.W. Jun, J.S. Choi, J. Cheon, Shape control of semiconductor and metal oxide nanocrystals through nonhydrolytic colloidal routes, Angew. Chem. Int. Ed. 45 (2006) 3414–3439.
[18] Y. Yin, A.P. Alivisatos, Colloidal nanocrystal synthesis and the organic–inorganic interface, Nature 437 (2005) 664–670.
[19] A.R. Tao, S. Habas, P.D. Yang, Shape control of colloidal metal nanocrystals, Small 4 (2008) 310–325.
[20] B. Wiley, Y. Sun, Y. Xia, Synthesis of silver nanostructures with controlled shapes and properties, Acc. Chem. Res. 40 (2007) 1067–1076.
[21] R. Narayanan, M.A. El-Sayed, Catalysis with transition metal nanoparticles in colloidal solution: nanoparticle shape dependence and stability, J. Phys. Chem. B 109 (2005) 12663–12676.
[22] C. Burda, X.B. Chen, R. Narayanan, M.A. El-Sayed, Chemistry and properties of nanocrystals of different shapes, Chem. Rev. 105 (2005) 1025–1102.
[23] M.P. Pileni, Control of the size and shape of inorganic nanocrystals at various scales from nano to macrodomains, J. Phys. Chem. C 111 (2007) 9019–9038.
[24] J. Park, J. Joo, S.G. Kwon, Y. Jang, T. Hyeon, Synthesis of monodisperse spherical nanocrystals, Angew. Chem. Int. Ed. 46 (2007) 4630–4660.
[25] G.A. Ozin, A.C. Arsenault, Nanochemistry: A Chemical Approach to Nanomaterials, RSC Publishing, Cambridge, 2005.
[26] A. Tesfai, B. El-Zahab, D.K. Bwambok, G.A. Baker, S.O. Fakayode, M. Lowry, I.M. Warner, Controllable formation of ionic liquid micro- and nanoparticles via a melt-emulsion-quench approach, Nano Lett. 8 (2008) 897–901.
[27] M. Green, P. Rahman, D. Smyth-Boyle, Ionic liquid passivated CdSe nanocrystals, Chem. Commun. (2007) 574–576.
[28] H.J. Chen, S.J. Dong, Self-assembly of ionic liquids-stabilized Pt nanoparticles into two-dimensional patterned nanostructures at the air–water interface, Langmuir 23 (2007) 12503–12507.
[29] S. Dai, Y.H. Ju, H.J. Gao, J.S. Lin, S.J. Pennycook, C.E. Barnes, Preparation of silica aerogel using ionic liquids as solvents, Chem. Commun. (2000) 243–244.
[30] Z.H. Li, Z.M. Liu, J.L. Zhang, B.X. Han, J.M. Du, Y.N. Gao, T. Jiang, Synthesis of single-crystal gold nanosheets of large size in ionic liquids, J. Phys. Chem. B 109 (2005) 14445–14448.
[31] A. Taubert, CuCl nanoplatelets from an ionic liquid–crystal precursor, Angew. Chem. Int. Ed. 43 (2004) 5380–5382.
[32] Y.J. Zhu, W.W. Wang, R.J. Qi, X.L. Hu, Microwave-assisted synthesis of single-crystalline tellurium nanorods and nanowires in ionic liquids, Angew. Chem. Int. Ed. 43 (2004) 1410–1414.
[33] Y. Wang, S. Maksimuk, R. Shen, H. Yang, Synthesis of iron oxide nanoparticles using a freshly-made or recycled imidazolium-based ionic liquid, Green Chem. 9 (2007) 1051–1056.
[34] Y. Wang, H. Yang, Oleic acid as the capping agent in the synthesis of noble metal nanoparticles in imidazolium-based ionic liquids, Chem. Commun. (2006) 2545–2547.
[35] B. Leger, A. Denicourt-Nowicki, A. Roucoux, H. Olivier-Bourbigou, Synthesis of bipyridine-stabilized, rhodium nanoparticles in non-aqueous ionic liquids: a new efficient approach for arene hydrogenation with nanocatalysts, Adv. Synth. Catal. 350 (2008) 153–159.
[36] P. Migowski, G. Machado, S.R. Texeira, M.C.M. Alves, J. Morais, A. Traverse, J. Dupont, Synthesis and characterization of nickel nanoparticles dispersed in imidazolium ionic liquids, Phys. Chem. Chem. Phys. 9 (2007) 4814–4821.
[37] L. Wang, L.X. Chang, B. Zhao, Z.Y. Yuan, G.S. Shao, W.J. Zheng, Systematic investigation on morphologies, forming mechanism, photocatalytic and photoluminescent properties of ZnO nanostructures constructed in ionic liquids, Inorg. Chem. 47 (2008) 1443–1452.
[38] J. Dupont, P.A.Z. Suarez, Physico-chemical processes in imidazolium ionic liquids, Phys. Chem. Chem. Phys. 8 (2006) 2441–2452.
[39] C. Wang, Y.L. Hou, J.M. Kim, S.H. Sun, A general strategy for synthesizing FePt nanowires and nanorods, Angew. Chem. Int. Ed. 46 (2007) 6333–6335.
[40] S. Peng, C. Wang, J. Xie, S.H. Sun, Synthesis and stabilization of monodisperse Fe nanoparticles, J. Am. Chem. Soc. 128 (2006) 10676–10677.
[41] K. Woo, J. Hong, S. Choi, H.W. Lee, J.P. Ahn, C.S. Kim, S.W. Lee, Easy synthesis and magnetic properties of iron oxide nanoparticles, Chem. Mater. 16 (2004) 2814–2818.
[42] R.M. Cornell, U. Schwertmann, The Iron Oxides: Structure, Properties, Reactions, Occurrences and Uses, 2nd ed., Wiley–VCH, Weinheim, 2003.
[43] J.W. Cheon, N.J. Kang, S.M. Lee, J.H. Lee, J.H. Yoon, S.J. Oh, Shape evolution of single-crystalline iron oxide nanocrystals, J. Am. Chem. Soc. 126 (2004) 1950–1951.
[44] D.L.A. deFaria, S.V. Silva, M.T. deOliveira, Raman microspectroscopy of some iron oxides and oxyhydroxides, J. Raman Spectrosc. 28 (1997) 873–878.

[45] M. Zubris, R.B. King, H. Garmestani, R. Tannenbaum, FeCo nanoalloy formation by decomposition of their carbonyl precursors, J. Mater. Chem. 15 (2005) 1277–1285.
[46] G.H. Tao, M. Zou, X.H. Wang, Z.Y. Chen, D.G. Evans, Y. Kou, Comparison of polarities of room-temperature ionic liquids using FT-IR spectroscopic probes, Aust. J. Chem. 58 (2005) 327–331.
[47] D.S. Jacob, V. Kahlenberg, K. Wurst, L.A. Solovyov, I. Felner, L. Shimon, H.E. Gottlieb, A. Gedanken, Sonochemical reaction of Fe(CO) with 1-methylimidazole in an ionic liquid: formation of (1-methylimidazole)(6)Fe-II (PF6)(2), Eur. J. Inorg. Chem. (2005) 522–528.
[48] J. Park, E. Lee, N.M. Hwang, M.S. Kang, S.C. Kim, Y. Hwang, J.G. Park, H.J. Noh, J.Y. Kini, J.H. Park, T. Hyeon, One-nanometer-scale size-controlled synthesis of monodisperse magnetic iron oxide nanoparticles, Angew. Chem. Int. Ed. 44 (2005) 2872–2877.
[49] N. Pradhan, H.F. Xu, X.G. Peng, Colloidal CdSe quantum wires by oriented attachment, Nano Lett. 6 (2006) 720–724.
[50] Z.Y. Tang, N.A. Kotov, One-dimensional assemblies of nanoparticles: preparation, properties, and promise, Adv. Mater. 17 (2005) 951–962.